Total Harmonic Distortion Measurement System of Electronic Devices up to 100MHz with Remarkable Sensitivity

Takanori Komuro [1) 3)] Shingo Sobukawa [2)] Haruo Kobayashi [3)] Hiroshi Sakayori [1)]
1) Agilent Technologies International Japan, Ltd., 9-1 Takakura-cho Hachioji-shi Tokyo 192-0033 Japan
Phone: 81-426-60-4519 Fax: 81-426-60-8429 E-mail: takanori_komuro@agilent.com
2) NF Corporation, 6-3-20 Tsunashima-Higashi Kouhoku-ku Yokohama-shi 223-8508 Japan
3) Dept. of Electronic Engineering, Gunma University, 1-5-1 Tenjin-cho Kiryu-shi 376-8515 Japan

Abstract - This paper describes a system for measuring total harmonic distortion (THD) components of signals from 1MHz to 100MHz at levels down to -130dBc. This system consists of a passive bandpass filter (BPF) and a passive band elimination filter (BEF) with carefully selected parts and that are mechanically sturdy. The BPF is used to create a pure sinusoidal signal input to the device under test (DUT), while the BEF removes the fundamental frequency component of the output signal- to overcome dynamic range limitations of the spectrum analyzer used to measure the output. We describe design concepts and implementation of these filters, as well as performance achieved and some measurement results using this system. Also through the measurement, a pure sine wave generation method and a linearity compensation method for the ADC using our BPF are proposed. The system can be used for high-precision measurement of AC linearity of electronic devices (such as OpAmps, ADCs, DACs) with several tens MHz range operation.

Keywords: LSI Testing, THD Measurement, Distortion, Bandpass Filter, Band Elimination Filter

I. Introduction

The measurement of THD of electronic devices has a long history [1]; for audio systems, the THD figure is used as a representation of AC linearity. THD measurement equipment for audio frequencies (up to 100kHz) is readily available commercially [2], and active filter technology can be used in such measurement equipment. However for MHz applications - like xDSL, cellular phone baseband signals, and HD video - it is very difficult to measure THD components that are 100dB below the carrier using active filter technology, because of noise and linearity limitations of active circuits.

Typical applications for THD measurements in the MHz range have been RF (radio frequency) systems which employ heterodyne technology; such RF applications require carrier signals in the MHz range - but the harmonic distortion of the signal is of less interest than in the above-mentioned audio example, because RF applications are mainly concerned with just the narrow band of modulation components around the carrier. Nevertheless, due to recent progress in semiconductor technology, wideband applications (i.e. DC to 100MHz) have become more important (Fig.1); for such applications, THD is a good index for representing linearity characteristics of analog circuits (like OpAmps, ADCs, DACs) [3]. However, THD testing of wideband devices over a wide dynamic range is currently quite difficult.

In this paper, we propose a system for measuring THD of analog circuits with very high resolution (down to -130dBc levels) and over a wide frequency range (1MHz to 100MHz). The system consists of a passive BPF and a passive BEF. The passive BPF is used to create a pure sine wave input to the DUT. The passive BEF is used to remove the fundamental frequency component from the DUT output signal without affecting the levels of the harmonics, so that the following spectrum analyzer can detect the harmonics with high precision. The filters are built with selected passive elements (L, C, R) for good linearity and noise performance. Section 2 describes the design concepts. Section 3 shows examples of THD measurement results using our proposed method. Section 4 provides conclusions.

II. Principle of THD Measurement

2.1 THD Measurement System

Fig.2 shows a diagram of our THD measurement system, wherein a pure sine wave signal is input to the

DUT and the output signal of the DUT is measured by a spectrum analyzer, to detect harmonic distortion that is generated in the DUT. Note that in Fig.2, THD is measured by the ratio of V_{dis} to $A * V_{in}$, and - in most cases - this ratio is very close to that of V_{dis} to V_{out}.

Since state-of-the-art commercial signal generators have output harmonic distortion levels of about -60dBc, we cannot use them directly as signal sources for high-resolution THD measurements. Thus filters are required to remove harmonics in the signal generator output, to enable THD measurements over a wider dynamic range. A BPF is desirable because it can remove low frequency noise (e.g. power-line noise). Also, the dynamic range of spectrum analyzers is typically about 80dBc, which restricts the dynamic range of THD measurements. To overcome this limitation, we use a BEF between the DUT and the spectrum analyzer; this BEF suppresses only the carrier signal (the large signal component at the fundamental signal frequency) while not affecting the level of very-small sideband signals (harmonic components). This enables the spectrum analyzer to measure very-small harmonic signals over a wide dynamic range. In actual measurement, a low noise amplifier was placed between the BEF and the spectrum analyzer to achieve the performance of -130dB level measurement. This low noise amplifier helps to reduce the equivalent noise level of the spectrum analyzer. Note that the low noise amplifier does not need to have critical performance of THD, because the largest component of the signal is removed through the BEF, and hence the low noise amplifier does not affect the distortion of the total system; it only has to have a flat frequency response in the frequency range of interest.

2.2 Band Pass Filter Design Concept

This subsection explains design concepts of the BPF and BEF in Fig.2. The BPF is made from passive components and Fig.3 shows a single stage of the BPF, where

$$L_1 = L_2(= L), \quad C_1 = C_2(= C), \quad L = CR^2. \quad (1)$$

The overall BPF consisits of several of this single-stage BPF, cascade-connected. The single-stage BPF (Fig.3) has the following characteristics:

Constant resistive output impedance : The output impedance of this filter is constant through the entire frequency range when eq.(1) holds; this enables us to connect many identical single-stage BPF in cascade. Also note that resistive termination does not affect the filter frequency response.

Low Q : The Q-value of the circuit in Fig.3 is relatively low, so the circuit is tolerant of variations in component parameter values. However the cascade connection of several stages enables the creation of a filter with sharp cutoff performance.

No loss in the passband (in theory): In reality there may be some loss, mainly caused by parasitic series resistance of inductors - but this loss can be easily compensated for, by calibration.

The impedance Z_{shunt} in Fig.3 is given by

$$Z_{shunt} = R + \left(j\omega L_2 \;||\; \frac{1}{j\omega C_2} \right) = \frac{R - \omega^2 LCR + j\omega L}{1 - \omega^2 LC}.$$

The series impedance Z_{series} in Fig.3 is expressed by

$$Z_{series} = R + j\omega L_1 + \frac{1}{j\omega C_1} = R + j\omega L + \frac{1}{j\omega C}.$$

Then we have the following filter transfer function:

$$H_{BPF}(j\omega) = \frac{Z_{shunt}}{Z_{series} + Z_{shunt}} = \frac{(K\omega_0)j\omega}{\omega_0^2 + j\omega(\omega_0/Q) - \omega^2}.$$

Here $K = 1,\ Q = 1,\ \omega_0 = \frac{1}{\sqrt{LC}}$. Note that $H_{BPF}(j0) = 0, \quad H_{BPF}(j\omega_0) = 1, \quad H_{BPF}(j\infty) = 0$. Also the network has a constant output impedance $Z_{out} = Z_{series} \;||\; Z_{shunt} = R$.

2.3 Band Elimination Filter Design

Our BEF in Fig.4 is designed using the same concept as the BPF one. Similarly eq.(1) holds, and the impedance Z_{shunt} in Fig.4 is given by

$$Z_{shunt} = R + j\omega L_3 + \frac{1}{j\omega C_3} = R + j\omega L + \frac{1}{j\omega C}.$$

The series impedance Z_{series} in Fig.4 is expressed by

$$Z_{series} = R + \left(j\omega L_4 \;||\; \frac{1}{j\omega C_4} \right) = \frac{R - \omega^2 LCR + j\omega L}{1 - \omega^2 LC}.$$

Then we have the following filter transfer function:

$$H_{BEF}(j\omega) = \frac{Z_{shunt}}{Z_{series} + Z_{shunt}} = \frac{K(\omega_0^2 - \omega^2)}{\omega_0^2 + j\omega(\omega_0/Q) - \omega^2}.$$

Table 1: Measured characteristics of 7 sets of BPF and BEF used in the THD measurement system.

	center freq. f_c	BPF loss @f_c	BEF notch @f_c	overall 2nd dist.	overall 3rd dist.	overall signal range
No.	MHz	dB	dB	dBc	dBc	Vp-p
1	1	-6.5	-110	-143	-135	5.0
2	2	-5.0	-119	-142	-146	5.0
3	5	-5.6	-110	-146	-146	5.0
4	10	-6.0	-106	-144	-142	5.0
5	20	-6.0	-104	-136	-150	5.0
6	50	-6.3	-110	-149	-153	3.1
7	100	-5.6	-106	-143	-129	3.3

Here $K = 1,\ Q = 1,\ \omega_0 = \frac{1}{\sqrt{LC}}$. Note that $H_{BEF}(j0) = 1,\ \ H_{BEF}(j\omega_0) = 0,\ \ H_{BEF}(j\infty) = 1,$ Also the network has a constant input impedance $Z_{in} = Z_{series} \parallel Z_{shunt} = R$. This BEF stage can be connected in series where its input impedance is kept constant.

2.4 Actual Filter Implementation

For a 10MHz BPF, 20 stages of the basic filter block (Fig.3) were connected in cascade, and the frequency response of this filter assembly was -100dB at 20MHz and -185dB at 30MHz. Fig.5 shows SPICE simulated gain characteristics of our BPF with 20 stages. Thanks to this high attenuation in the stop band, a pure sine wave signal can be extracted from a square wave for the input signal. Fig.6 shows a photo of our BPF, and its length is 345 mm, width is 75mm, while thickness is 28mm.

Remarks: (i) The distortion caused by filter parts is an important concern. In most cases, non-linearity of magnetic cores of inductors causes distortion, and - in general - physically large inductors with low-permeability cores generate less distortion than small - e.g. surface-mount - inductors.

(ii) The mounting of parts is also important. Any magnetic coupling between stages reduces attenuation in the stop band. To alleviate this problem, we mounted filter components in cavities of a cast aluminum block; such construction also helps minimize vibration-induced noise.

The design of the BEF is similar to that of the BPF. But in this case a three-stage cascade connection is sufficient, because the BEF only has to reduce the ratio between the fundamental signal and the harmonics to a level that the spectrum analyzer can handle. The important parameters for the BEF are the gain response at 2nd and 3rd harmonic frequencies, because, due to the low Q of the BEF, the frequency response at those frequencies shows some attenuation. Fig. 7 shows a photo of our BEF, and its length of the BEF is 105mm, width is 75mm, while thickness is 28mm.

We made 7 kinds of filter sets with different center frequencies, and each filter has *fixed* frequency response. Table 1 shows the measured characteristics of the BPF and BEF. The values in Table 1 are compensated ones for the attenuation of the BEF, and the overall performance was measured with connecting BPF and BEF directly. Note that the signal level of 3Vp-p in Table-1 is large enough for present-day devices, and this value can be obtained with 50-ohm termination.

III. Measurement Examples

3.1 Using Square Wave Signal as BPF Input

For ADC THD measurement, we have to be aware of input-signal phase noise. We propose feeding a square wave from a quartz generator (whose phase noise is quite low) directly into the BPF to generate a low phase-noise sinusoidal signal; voltage noise like thermal noise can be translated into phase noise by the factor of the inverse of signal slew rate. The 3rd harmonics of a square wave is -10dBc, and to achieve the THD level of -130dBc at the BPF output, we really need the attenuation of 3rd order harmonics to -120dB, and therefore we use 20 stages in series as basic construction of the BPF.

We also need a good isolation between the input and output of the BPF; we used a rigid shielding case for mounting of filter components. It is also important to keep the impedance of top cover of the shielding case low. Fig. 8 shows the model of coupling between the input and output of the BPF through the shielding case cover. For explanation, we assume that the center frequency of BPF is 10MHz, and we calculate the attenuation at 30MHz. Using assumed value of parasitic components described in Fig.8, L

of 10nH gives -92dBc level feed-through at 30MHz, while R of 0.2 ohm gives -110dBc level. So in order to achieve the attenuation of -120dB, we have to keep these values low enough. In Figs. 5 and 6, we see many screw holes, which are prepared for keeping the impedance of caver low enough.

3.2 Photo MOS Relay Switch

Photo MOS relay switches are extensively used in LSI testers, which require highly-linear switches. For such applications, we evaluated the linearity of a photo MOS relay using our system; Figs. 9 and 10 show its distortion measurement results. Its measured distortion level is low enough for most LST tester applications; we see in Figs.9 and 10, that our proposed method clearly detects the distortion. Colleagues with material and fabrication expertise are now considering possible causes of the distortion, so the proposed system is helping them understand physics-of-materials phenomena.

3.3 ADC with Wideband S/H Circuit

In this subsection we propose a method for using our BPF to compensate for distortion of the ADC with S/H circuit. By using our BPF to obtain a pure sine wave, we can measure THD of the system by performing FFT on the digital output data. Fig.12(a) shows the measurement results of ADC with wideband S/H. The input signal frequency is 100MHz. Since the above method with our BPF can create a pure sinusoidal input, almost all of the measured distortion is due to the DUT itself. Then we measured the DC characteristics of the ADC with S/H by using a DC voltage source and a precision DC voltmeter, to obtain a graph like Fig. 11. Then we obtain a polynomial expression which approximates the DC characteristics in Fig.11. We also obtain another polynomial expression which is the inverse function of the DC characteristics polynomial expression; it is stored in a look-up table, and the output digital data of the ADC with S/H are applied to it. Then digital calculation provides compensated ADC outputs with improved linearity.

Figs.12(a),(b) show the effectiveness of the proposed linearity compensation method for the ADC with S/H circuit. Fig.12(a) shows the measured output spectrum (obtained by FFT of ADC output data) of the ADC with S/H circuit for a 100MHz sinusoidal input signal while Fig.12(b) shows the spectrum after compensation. We see that applying this compensation method reduces the THD level of the 100MHz signal by 18dB.

In this case, the data for compensation were taken through the DC characteristics measurement, which means that, main cause of the distortion in the system at 100MHz is the same as that at DC; this relationship between ADC DC linearity and AC linearity at 100MHz is one of examples for wide-band applications described in section 1.

IV. Conclusion

We have addressed the importance of THD measurement of electronic devices at frequencies higher than typical audio applications, and we have proposed a THD measurement system for analog input and/or analog output devices at frequencies of several tens of MHz. The proposed system uses passive BPF and BEF, and we described their design and implementation. The proposed system can measure THD components down to -120dBc or less over a frequency range from 1MHz to 100MHz, which has not been achieved with the other methods (we believe that this performance will be sufficient for our LSI tester applications for the next ten years). By paying attention to component selection and mounting, we have created a mechanically-sturdy measurement system with good reliability and repeatability. We have described examples of THD measurement which verify the effectiveness of using the proposed system. We have also shown that even classical subjects like THD measurement or passive filters, have many new findings inside when we enter into much deeper level than ever before. Furthermore, apart from its electrical applications, this system also has the potential to be used as a very sensitive detector of physical phenomena-with “ ppm level ” resolution.

Acknowledgment We thank our managers as well as H. Kakitani, K. Wilkinson and M. Kono.

References

[1] HP 8903B Audio Analyzer Operation and Calibration Manual, 4th ed., Hewlett-Packard Company, Spokane, WA (1989).

[2] APWIN System Two Cascade User's Manual, Audio Precision, Inc., Beaverton, OR (2001).

[3] P. Wambacq, W. Sansen, Distortion Analysis of Analog Integrated Circuits, Kluwer Academic Publishers (2002).

[4] H. Kobayashi, et. al., "Sampling Jitter and Finite Aperture Time Effects in Wideband Data Acquisition Systems," *IEICE Trans. on Fundamentals,* vol. E85-A, no. 2, pp.335-346 (Feb. 2002).

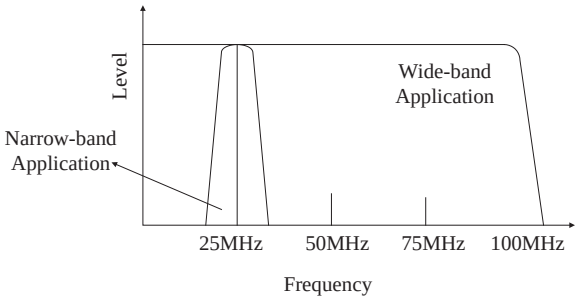

Fig.1: Signal bands for narrow-band and wide-band applications.

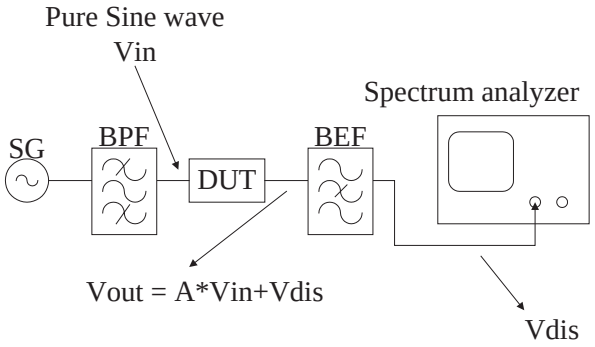

Fig.2: Our THD measurement system.

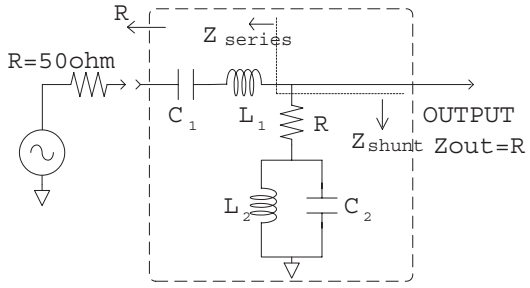

Fig.3: Single-stage of BPF with constant output impedance.

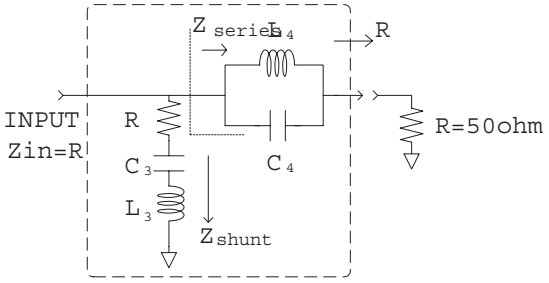

Fig.4: Single stage of BEF with constant input impedance.

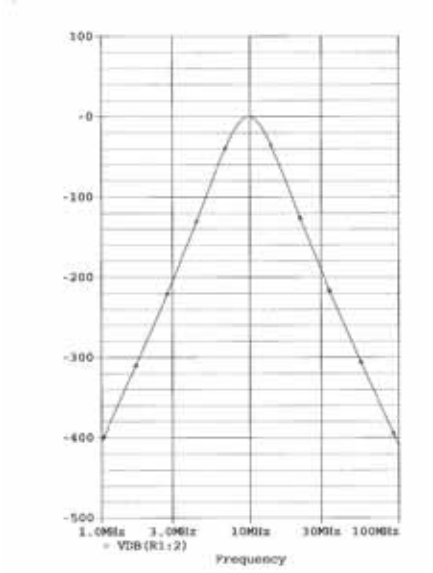

Fig.5: SPICE simulated gain characteristics of BPF with 20 stages with the center frequency of 10MHz. L=0.82uH, C=318pF and R=51Ω.

Fig.6: A photo of our BPF. Components are stud-mounted in cavities of a cast-aluminum block. The holes shown are prepared for screw up.

Fig.7: A photo of our BEF without cover.

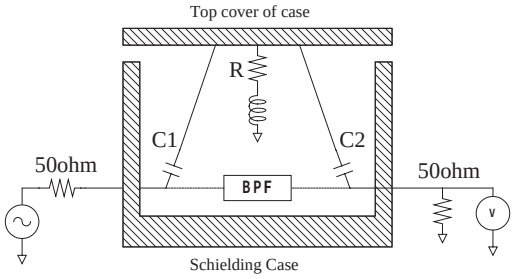

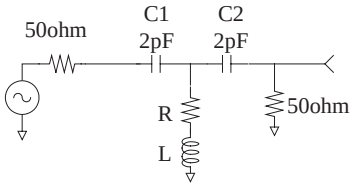

Fig.8: Model of coupling between BPF input and output.

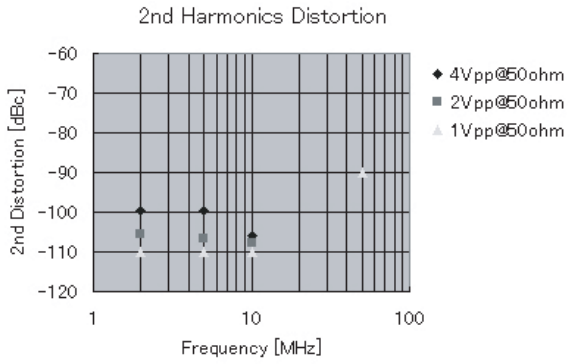

Fig.9: 2nd-order distortion of a photo MOS relay measured with our system.

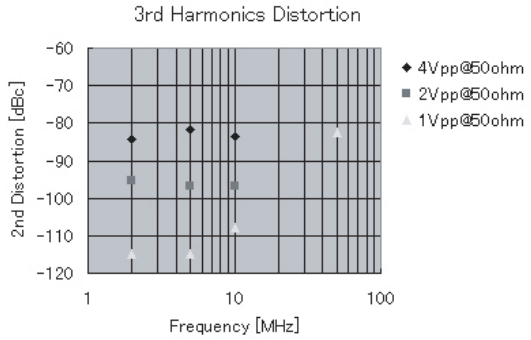

Fig.10: 3rd-order distortion of a photo MOS relay measured with our system.

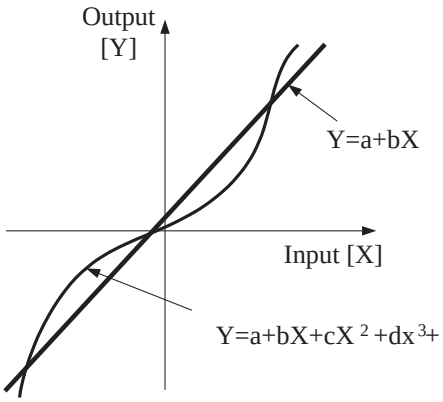

Fig.11: The principle of the ADC linearity improvement method.

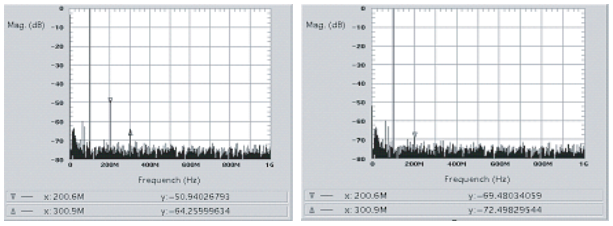

(a) (b)

Fig.12: (a) Distortion of ADC and S/H without compensation THD=-48.5dBc @ 100MHz. (b) With compensation THD=-66.8dBc @ 100MHz.